Journal of Sound and Vibration (2002) **255**(4), 615–633
doi:10.1006/jsvi.2001.4181, available online at http://www.idealibrary.com on IDEAL®

INTERACTION OF A SPHERICAL SHOCK WAVE AND A SUBMERGED FLUID-FILLED CIRCULAR CYLINDRICAL SHELL

S. IAKOVLEV

Department of Engineering Mathematics, Dalhousie University, Halifax, Nova Scotia, Canada B3J 2X4. E-mail: serguei.iakovlev@dal.ca

(*Received* 24 *August* 2001, *and in final form* 16 *November* 2001)

The complete three-dimensional interaction between a spherical shock wave and a submerged fluid-filled elastic circular cylindrical shell is considered. A hybrid analytical–numerical solving procedure is established. An exact analytical solution in the form of double Fourier series with time-depending coefficients is obtained for the hydrodynamic pressure. Displacements of a shell are approached analytically to reduce the problem to a set of systems of ordinary differential equations, which are treated numerically. Detailed analysis of the interaction is performed with emphasis given to the stress–strain state. A few important features of the interaction process have been found. In particular, it has been shown that the interior fluid not only substantially affects the magnitude of displacements and stresses, but also dramatically changes the nature of the interaction. It has been found that the absolute maximum of stresses can neither be caused by a direct action of a shock wave nor by a constructive superpose of elastic waves in the shell, but by the pressure wave propagating in the interior fluid. This fact seems to be of essential importance for engineering applications, especially when safety is a primary design concern. Another important result is that the maximum stresses are attained at large times, which makes use of early time asymptotics leading to incorrect results. The proposed semi-analytical approach seems to be computationally attractive and suitable for extensive numerical simulations.

1. INTRODUCTION

The interaction of hydrodynamic loads with circular cylindrical structures has been of substantial interest over the last few decades. Two main groups of problems have been addressed: low-frequency loading, with the ocean waves as the best studied case, and high-frequency loading, where shock waves, earthquake excitations, and acoustic pulses are of primary interest. In the present paper, the second class of the problems is addressed, and the most complex 'three-media' case of the contact (exterior fluid–shell–interior fluid) is investigated.

Referring to the existing literature, the interaction of a plane shock wave and a circular cylindrical shell was first approached by Mindlin and Bleich [1]. Their solution involved a few significant simplifications, and was only valid for the beginning of the process. Haywood [2] considered interaction with the same plane shock wave but introduced another solution, which allowed to address larger times. However, it still involved some 'early time' simplifications. A complete exact solution for this two-dimensional problem was obtained by several authors. Here we will mention works of Geers [3], Huang [4],

0022-460X/02/$35.00

Mnev and Pertsev [5], and Pertsev and Platonov [6]. All the authors used the same approach based on the Laplace–Fourier transform technique, and obtained an analytical solution in the form of Fourier series with time-dependent coefficients.

The interaction of a completely submerged circular cylindrical shell with three-dimensional loads, such as the spherical shock waves, is the most "geometrically" complex case, and it was first addressed in early 1970s. Huang and Wang [7] presented a solution using the Laplace–Fourier transform technique, and applied a numerical procedure to calculate the inverse transforms. Pertsev and Platonov [6] discussed diffraction and radiation problems in some details using the same technique to obtain expressions for transforms, and an analytical procedure to perform the inverse transform.

The problem of loading on a shell filled with an acoustic media was addressed first by Peralta and Reynor [8]. They considered a fluid-filled shell submersed in an acoustic media and subjected to a plane step pressure pulse, and made use of the Fourier–Laplace transform to find a solution which was only valid for the early stage of the process. Tang [9] studied the dynamic response of a fluid-filled shell to a load moving in the axial direction with a constant speed. He used simplified equations of the axisymmetric motion of a thin-walled shell (Timoshenko's equations of beam vibrations), therefore the performed analysis was one-dimensional. King and Frederick [10] considered elastic waves propagating in a fluid-filled cylindrical shell. Again, the problem was treated as axially symmetric, and only an early-time stage was addressed. It seems that the most advanced study of the problem was performed by Carpenter and Berger [11]. They investigated loading on a semi-infinite fluid-filled shell governed by the Love–Timoshenko shell equations, and containing a fluid satisfying the three-dimensional wave equation. The authors used the Hankel–Fourier–Laplace transform to obtain a solution in an analytical form, and then applied a numerical inversion procedure to find the displacements. Only a simple axisymmetric periodic load was considered, and stresses were not addressed at all.

Thus, to the best of the author's knowledge, it seems that the problem of the complete interaction between an essentially three-dimensional load such as a spherical shock wave, and an elastic circular cylindrical shell both filled with fluid and submerged in another one, has not been addressed yet. Also, most of the above-mentioned works gave solutions in the form of multiple integral transforms which appears to be not very useful for analysis based on those solutions. Hence, it is very desirable to obtain inverse transforms in an analytical form to make the results more practically applicable.

In this paper, we are using a semi-analytical approach based on separation of variables (space co-ordinates), the Laplace transform (time), and numerical treatment of the reduced system for shell displacements (finite difference approach). The proposed methodology differs from most of the previously published works in a way the Laplace transform is applied. Here the transform is used to obtain an analytical solution for a 'hydrodynamic' part of the problem, and pressure is obtained in the form of double Fourier series with time-dependent coefficients. Numerical treatment of the 'elastic' part is performed in the time domain. Other researchers preferred to obtain displacements in the form of integral transforms, and then applied numerical inversion at the very end. Their approach may seem to be more straightforward, and the question arises: does the proposed method have any advantageous over the previously published works? The author believes that it does.

In the proposed method, the numerical inverse of the Laplace transform is applied only once to calculate the response functions. The total pressure is expressed in terms of these functions in the integral form. The response functions are uniform for all the problems of the same geometry, and do not depend on the parameters of the system. Thus, the most sophisticated (and time-consuming) 'inversion' part is localized in calculating the response functions, and the rest of the solution is just a technical issue involving numerical

integration and one-dimensional finite difference approximation. At this point, it is very easy to change the system's parameters and perform calculations for a large number of different systems. For example, varying the thickness of a shell and/or density of the fluids would affect only the final part of the solving procedure, and it would only take an insignificant fraction of total computational time. In contrast, if one uses the alternative method (inverse transformation at the end), even a change of one parameter would cause the necessity to calculate many inverse transforms all over again. In this case, computational efforts can become unreasonable when the analysis of large number of different systems is a goal. All the above-mentioned makes the author believe that the proposed method is suitable for extensive numerical simulations and is more computationally attractive than the one in common use.

We should note here that, following the common trend in engineering mathematics, numerical methods have been gaining more popularity. Innumerous numerical codes have been produced, from relatively simple ones aimed at analyzing a particular problem, to universal supercomputer-oriented industrial codes. Some researchers have been focused on the study of the shock waves propagation and diffraction over a rigid fixed cylindrical structure (e.g., references [12, 13]), while others have been addressing a 'hydroelastical' aspect of fluid–shell interaction, developing efficient solvers for coupled equations of a shell and fluid(s).

There is no need of emphasizing the importance of numerical analysis of structures. The present paper is not an attempt to compete with numerical codes in any way, but just another approach to the complex multi-media problem of hydroelasticity. The obtained solution is 'exact', and hence it may be successfully used for validation of numerical codes. Even in this capacity, an analytical treatment of the problem deserves attention. Besides, for a wide variety of loads (especially for not very intensive ones) the proposed solution will give results which are very close to the real values of physical quantities.

2. MATHEMATICAL FORMULATION

We are considering a thin elastic circular cylindrical shell submerged in and filled with homogeneous, inviscid, linearly compressible fluid. The radius of the shell is A, and the thickness is H_0. The shell is subjected to a spherical shock wave. Let (X, θ, R) be a cylindrical co-ordinates system based on the axis of the shell, and let $(0, 0, D)$ be co-ordinates of the source of the shock wave. The geometry of the problem is shown in Figure 1.

The fluids are governed by the wave equation for the fluid potential Φ which is

$$\nabla^2 \Phi_e = \frac{1}{C_e^2} \frac{\partial^2 \Phi_e}{\partial T^2} \tag{1}$$

for the exterior fluid, and

$$\nabla^2 \Phi_i = \frac{1}{C_i^2} \frac{\partial^2 \Phi_i}{\partial T^2} \tag{2}$$

for the interior one. Here, Φ_e and Φ_i are the potentials of the exterior and interior fluids, respectively, C_e and C_i the sound speeds in the exterior and interior fluids, and T the time. Hydrodynamic pressure and potential are connected by

$$P_e = -\rho_e \frac{\partial \Phi_e}{\partial T} \quad \text{and} \quad P_i = -\rho_i \frac{\partial \Phi_i}{\partial T} \tag{3}$$

for the exterior and interior fluids, respectively, with ρ_e and ρ_i being densities of the fluids.

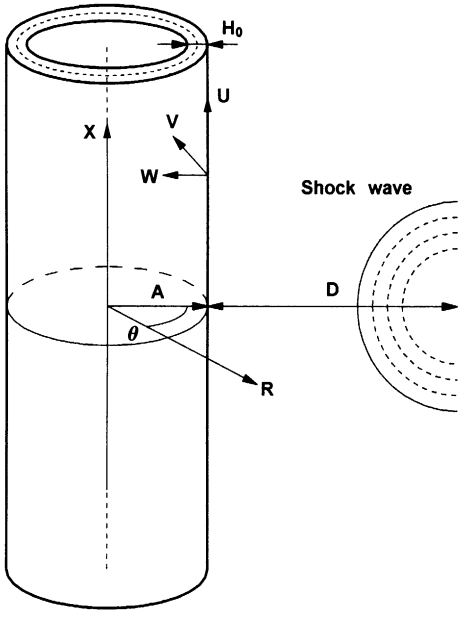

Figure 1. Geometry of the problem.

We assume the shell to be thin which means that its thickness is much smaller than the radius. Also, we take into account both the stretching (expanding) energy and the bending one. In this case, we can use Love's expression for the strain energy per unit area of the shell [14]:

$$\frac{EH_0}{2(1-\nu^2)}\{\varepsilon_1^2+\varepsilon_2^2+2\nu\varepsilon_1\varepsilon_2+\tfrac{1}{2}(1-\nu)\Omega^2 + K^2A^2(\kappa_1^2+\kappa_2^2+2\nu\kappa_1\kappa_2+2(1-\nu)\tau^2)\}, \tag{4}$$

along with the known expression for the kinetic energy per unit area,

$$\frac{1}{2}\rho_s H_0\left\{\left(\frac{\partial U}{\partial T}\right)^2+\left(\frac{\partial V}{\partial T}\right)^2+\left(\frac{\partial W}{\partial T}\right)^2\right\}, \tag{5}$$

to derive equations of shell dynamics using Hamilton's principle. Here,

$$\varepsilon_1=\frac{\partial U}{\partial X},\quad \varepsilon_2=\frac{1}{A}\left(\frac{\partial V}{\partial\theta}-W\right),\quad \Omega=\frac{\partial V}{\partial X}+\frac{1}{A}\frac{\partial U}{\partial\theta}, \tag{6}$$

$$\kappa_1=\frac{\partial^2 W}{\partial X^2},\quad \kappa_2=\frac{1}{A^2}\left(\frac{\partial^2 W}{\partial\theta^2}-\frac{\partial V}{\partial\theta}\right),\quad \tau=\frac{1}{A}\left(\frac{\partial^2 W}{\partial\theta\partial X}-\frac{\partial V}{\partial X}\right), \tag{7}$$

where U, V, and W are the X, θ, and R components of the displacement of the middle surface of the shell, ρ_s is density of the shell material, E is Young's modulus of the shell material, ν is the Poisson ratio of the shell material, and $K^2=H_0^2/12$. Note that, unlike in Love's work, we consider an inward normal for the 'elastic' part of the problem and an outward one for the 'hydrodynamic' part ('$-$' instead of '$+$' in the expression for ε_2).

The boundary conditions on the contract surface are

$$\left.\frac{\partial \Phi_e}{\partial R}\right|_{R=A} = -\frac{\partial W}{\partial T}, \qquad \left.\frac{\partial \Phi_i}{\partial R}\right|_{R=A} = -\frac{\partial W}{\partial T}, \tag{8}$$

the condition at the axis of the shell is

$$|\Phi_i|_{R=0}| < \infty, \tag{9}$$

and at the infinity we have

$$\lim_{R\to\infty} \Phi_e = 0. \tag{10}$$

Because of the infinite length of the shell, the boundary conditions with respect to X can be formulated as

$$\Phi|_{X=\pm X_0} = 0, \tag{11}$$

$$\left.\frac{\partial U}{\partial X}\right|_{X=\pm X_0} = 0, \quad V|_{X=\pm X_0} = 0, \quad W|_{X=\pm X_0} = 0, \quad \left.\frac{\partial^2 W}{\partial X^2}\right|_{X=\pm X_0} = 0, \tag{12}$$

where X_0 is large enough for the time interval we are interested to address. The potential and the displacements are to be periodical with respect to θ. All the initial conditions are zero.

Let us now introduce the following dimensionless quantities (the system A, C_e, and ρ_e is chosen as a 'basis'):

$$x = \frac{X}{A}, \quad r = \frac{R}{A}, \quad h_0 = \frac{H_0}{A}, \quad x_0 = \frac{X_0}{A}, \quad u = \frac{U}{A}, \quad v = \frac{V}{A}, \quad w = \frac{W}{A}, \tag{13}$$

$$d = \frac{D}{A}, \quad t = \frac{TC_e}{A}, \quad k^2 = \frac{K_0^2}{A^2}, \quad \bar{E} = \frac{E}{\rho_e C_e^2}, \quad c_i = \frac{C_i}{C_e}, \quad c_s = \frac{C_s}{C_e}, \tag{14}$$

$$\bar{\rho}_i = \frac{\rho_i}{\rho_e}, \quad \bar{\rho}_s = \frac{\rho_s}{\rho_e}, \quad \phi_e = \frac{\Phi_e}{C_e A}, \quad \phi_i = \frac{\Phi_i}{C_e A}, \quad p_e = \frac{P_e}{\rho_e C_e^2}, \quad p_i = \frac{P_i}{\rho_e C_e^2}, \tag{15}$$

where C_s is the sound speed in the shell material defined as $C_s = \sqrt{E/(\rho_s(1-\nu^2))}$.

Now we have

$$\varepsilon_1 = \frac{\partial u}{\partial x}, \quad \varepsilon_2 = \left(\frac{\partial v}{\partial \theta} - w\right), \quad \Omega = \frac{\partial v}{\partial x} + \frac{\partial u}{\partial \theta}, \tag{16}$$

$$\kappa_1 = \frac{\partial^2 w}{\partial x^2}, \quad \kappa_2 = \left(\frac{\partial^2 w}{\partial \theta^2} - \frac{\partial v}{\partial \theta}\right), \quad \tau = \left(\frac{\partial^2 w}{\partial \theta \partial x} - \frac{\partial v}{\partial x}\right). \tag{17}$$

If we decompose the potential in the exterior fluid as

$$\phi_e = \phi_0 + \phi_d + \phi_r, \tag{18}$$

where ϕ_0 is a known incident potential, ϕ_d is a diffracted potential, and ϕ_r is a radiated potential, three initial boundary value problems can be formulated for the unknown components of the potential. ϕ_d, ϕ_r, and ϕ_i must satisfy the zero boundary condition at $x = \pm x_0$, periodicity conditions with respect to θ, zero initial conditions, but different boundary conditions with respect to the radial co-ordinate.

The diffracted potential ϕ_d is to satisfy the equation

$$\nabla^2 \phi_d = \frac{\partial^2 \phi_d}{\partial t^2}, \tag{19}$$

boundary condition at the shell surface

$$\left.\frac{\partial \phi_d}{\partial r}\right|_{r=1} = -\left.\frac{\partial \phi_0}{\partial r}\right|_{r=1}, \tag{20}$$

and the zero boundary condition at infinity.

The radiated potential ϕ_r is to satisfy the same equation as ϕ_d, the same zero condition at infinity, and the boundary condition at the shell surface in the form

$$\left.\frac{\partial \phi_r}{\partial r}\right|_{r=1} = -\frac{\partial w}{\partial t}. \tag{21}$$

Finally, the potential in the interior fluid must satisfy the equation

$$\nabla^2 \phi_i = \frac{1}{c_i^2}\frac{\partial^2 \phi_i}{\partial t^2}, \tag{22}$$

the contact surface boundary condition

$$\left.\frac{\partial \phi_i}{\partial r}\right|_{r=1} = -\frac{\partial w}{\partial t}, \tag{23}$$

and must be bounded at the axis of the shell

$$|\phi_i|_{r=0}| < \infty. \tag{24}$$

Equations for the displacements will be derived later on.

Before we turn to the solution, let us briefly address the spherical shock waves. It can be shown (e.g., reference [15]) that the potential of a shock wave with exponentially decaying pressure behind its front has the form

$$\phi_0 = \frac{\alpha\lambda}{d_1}(\mathrm{e}^{-(t-d_1+d-1)/\lambda} - 1)\, H(t - d_1 + d - 1), \tag{25}$$

where λ is a parameter of exponential decay, α is a normalizing parameter to provide realistic magnitudes of the pressure in the front of the shock wave, $d_1 = \sqrt{d^2 + x^2 + 1 - 2d\cos\theta}$ is the distance between the source of the shock wave and the point (x, θ) at the surface of the shell, and

$$H(z) = \begin{cases} 1, & z \geqslant 0, \\ 0, & z < 0. \end{cases} \tag{26}$$

Note that in this formulation, we consider the moment of contact between the shock wave and the shell as initial.

The parameters α and λ depend on the distance d, explosive material, and some other factors. Exact values can be adopted from the theory of underwater shock waves [15] for each particular case. For example, if we address a typical underwater explosion, for $d = 1{\cdot}2$ we will have $\lambda = 0{\cdot}121$ and $\alpha = 0{\cdot}0203$, whereas for $d = 5{\cdot}0$, we will arrive at $\lambda = 0{\cdot}184$ and $\alpha = 0{\cdot}00403$.

3. HYDRODYNAMIC PRESSURE

In this section, we will derive analytical expressions for the total hydrodynamic pressure acting at the shell surface. If we assign that pressure p_0 corresponds to the potential ϕ_0, p_d to

ϕ_d, p_r to ϕ_d, and p_i to ϕ_i, the total pressure at the shell surface will be

$$p = (p_0 + p_d + p_r - p_i)|_{r=1}. \tag{27}$$

Let us apply the Laplace transform with respect to time to equation (19) written in cylindrical co-ordinates,

$$\frac{\partial^2 \phi_d^L}{\partial r^2} + \frac{1}{r}\frac{\partial \phi_d^L}{\partial r} + \frac{\partial^2 \phi_d^L}{\partial x^2} + \frac{1}{r^2}\frac{\partial^2 \phi_d^L}{\partial \theta^2} - s^2 \phi_d^L = 0. \tag{28}$$

Here, L denotes the Laplace transform of a function and s the parameter of the transform.

Separation of variables with respect to the space co-ordinates gives the general solution of equation (28) as

$$\phi_d^L = \sum_{m=0}^{\infty} \sum_{n=0}^{\infty} G_{mn}(s) K_n(r\beta_m(s)) \cos(\bar{m}x) \cos(n\theta), \tag{29}$$

where $K_n(s)$ is the modified Bessel function of the second kind of order n, $G_{mn}(s)$ is an arbitrary function of s, $\beta_m(s) = \sqrt{\bar{m}^2 + s^2}$, and $\bar{m} = (2m + 1)\,(2x_0)^{-1}\,\pi$. Let us decompose $\partial\phi_0/\partial r\,|_{r=1}$ into the Fourier series

$$\left.\frac{\partial \phi_0}{\partial r}\right|_{r=1} = \sum_{m=0}^{\infty} \sum_{n=0}^{\infty} b_{mn}(t) \cos(\bar{m}x) \cos(n\theta), \tag{30}$$

where

$$b_{mn}(t) = \frac{\Delta_{mn}}{\pi x_0} \int_0^{\pi} \int_0^{x_0} \left.\frac{\partial \phi_0}{\partial r}\right|_{r=1} \cos(\bar{m}x) \cos(n\theta)\, \mathrm{d}x\, \mathrm{d}\theta, \tag{31}$$

and $\Delta_{m0} = 2$, while $\Delta_{mn} = 4$, $n > 0$. If we make use of the boundary condition (20), G_{mn} will take the form

$$G_{mn}(s) = -\frac{b_{mn}^L(s)}{\beta_m(s) K_n'(\beta_m(s))}. \tag{32}$$

Now, taking into account the connection (3) between pressure and potential, the diffraction pressure at the shell surface may be obtained in the form

$$p_d|_{r=1} = -\sum_{m=0}^{\infty} \sum_{n=0}^{\infty} \left\{ b_{mn}(t) + \int_0^t b_{mn}(\tau) \dot{\psi}_{mn}(t-\tau) \mathrm{d}\tau \right\} \cos(\bar{m}x) \cos(n\theta). \tag{33}$$

Here dot denotes the differentiation, and $\psi_{mn}(t)$ are the response functions of the 'exterior' part of the problem with the Laplace transforms given by

$$\psi_{mn}^L(s) = -\frac{K_n(\beta_m(s))}{\beta_m(s) K_n'(\beta_m(s))}, \tag{34}$$

where the prime denotes the first derivative. As one can see now, the diffraction pressure is known as soon as the response functions are calculated.

If we decompose the normal displacement w as

$$w = \sum_{m=0}^{\infty} \sum_{n=0}^{\infty} w_{mn}(t) \cos(\bar{m}x) \cos(n\theta), \tag{35}$$

and take into account the boundary conditions (21) and (23), both radiation pressure and the pressure in the interior fluid can be easily derived:

$$p_r|_{r=1} = -\sum_{m=0}^{\infty}\sum_{n=0}^{\infty}\left\{\int_0^t \ddot{w}_{mn}(\tau)\psi_{mn}(t-\tau)\,\mathrm{d}\tau\right\}\cos(\bar{m}x)\cos(n\theta), \tag{36}$$

$$p_i|_{r=1} = \bar{\rho}_i c_i^2 \sum_{m=0}^{\infty}\sum_{n=0}^{\infty}\left\{\int_0^{c_i t} \ddot{w}_{mn}(\tau)\xi_{mn}(c_i t-\tau)\,\mathrm{d}\tau\right\}\cos(\bar{m}x)\cos(n\theta). \tag{37}$$

Here, ξ_{mn} are the response functions of the 'interior' part of the problem. The Laplace transforms of ξ_{mn} are given by

$$\xi_{mn}^L(s) = \frac{\mathrm{I}_n(\beta_m(s))}{\beta_m(s)\mathrm{I}_n'(\beta_m(s))}, \tag{38}$$

where $\mathrm{I}_n(s)$ is the modified Bessel function of the first kind of order n. Again, the problem is reduced to calculation of the response functions.

Finally, if we decompose the incident pressure at the shell surface in a Fourier series

$$p_0|_{r=1} = \sum_{m=0}^{\infty}\sum_{n=0}^{\infty} a_{mn}(t)\cos(\bar{m}x)\cos(n\theta), \tag{39}$$

where

$$a_{mn}(t) = \frac{\Delta_{mn}}{\pi x_0}\int_0^{\pi}\int_0^{x_0} p_0|_{r=1}\cos(\bar{m}x)\cos(n\theta)\,\mathrm{d}x\,\mathrm{d}\theta, \tag{40}$$

the total hydrodynamic pressure (27) will take the form

$$p = \sum_{m=0}^{\infty}\sum_{n=0}^{\infty} p_{mn}(t)\cos(\bar{m}x)\cos(n\theta), \tag{41}$$

where

$$p_{mn}(t) = a_{mn}(t) - b_{mn}(t) - \int_0^t b_{mn}(\tau)\dot{\psi}_{mn}(t-\tau)\,\mathrm{d}\tau$$
$$-\int_0^t \ddot{w}_{mn}(\tau)\psi_{mn}(t-\tau)\,\mathrm{d}\tau - \bar{\rho}_i c_i^2\int_0^{c_i t}\ddot{w}_{mn}(\tau)\xi_{mn}(c_i t-\tau)\,\mathrm{d}\tau. \tag{42}$$

4. RESPONSE FUNCTIONS

It is easy to show that the response functions ψ_{mn} and ξ_{mn} can be expressed as

$$\psi_{mn}(t) = \psi_n(t) - \bar{m}\int_0^t \psi_n(\sqrt{t^2-\tau^2})\,\mathrm{J}_1(\bar{m}\tau)\,\mathrm{d}\tau, \tag{43}$$

$$\xi_{mn}(t) = \xi_n(t) - \bar{m}\int_0^t \xi_n(\sqrt{t^2-\tau^2})\,\mathrm{J}_1(\bar{m}\tau)\,\mathrm{d}\tau, \tag{44}$$

where J_1 is the Bessel function of the first order, and ψ_n and ξ_n are the response functions of the corresponding two-dimensional problems with the Laplace transforms defined by

$$\psi_n^L(s) = -\frac{K_n(s)}{sK_n'(s)} \quad \text{and} \quad \xi_n^L(s) = \frac{\mathrm{I}_n(s)}{s\mathrm{I}_n'(s)}. \tag{45}$$

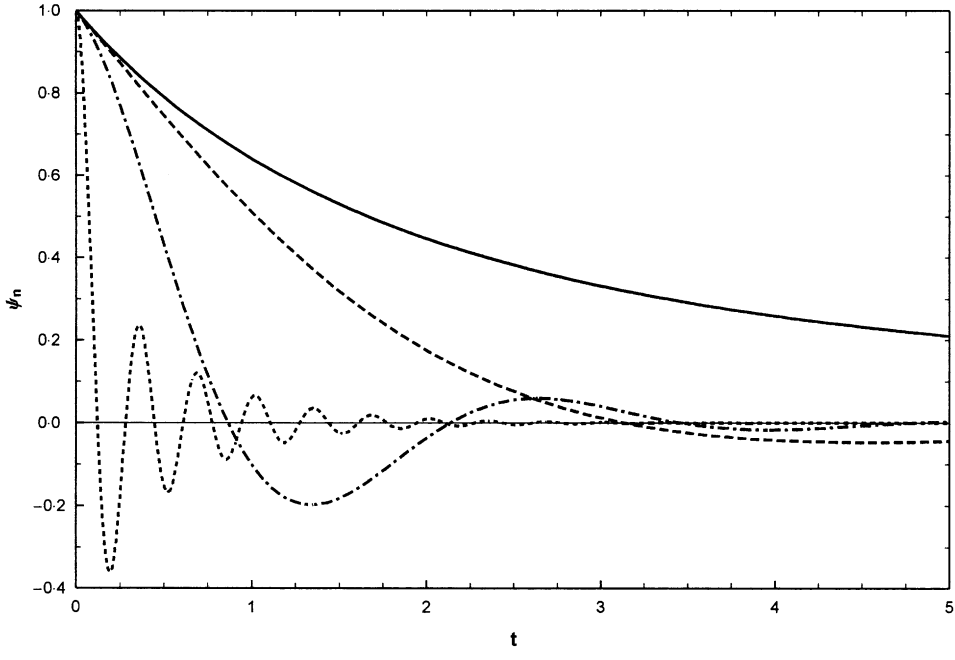

Figure 2. Functions $\psi_n(t)$ for various n: ——, $\psi_0(t)$; – – –, $\psi_1(t)$; – · –, $\psi_3(t)$; - - - -, $\psi_{20}(t)$.

The functions ψ_n have been calculated using a numerical method based on the reduction of Mellin's integral for ψ_n to a Fourier cosine integral. All the details can be found in reference [16]. Here we will just mention the basic properties of the functions ψ_n:

$$\psi_n|_{t=0} = 1, \quad \left.\frac{\partial \psi_n}{\partial t}\right|_{t=0} = -\frac{1}{2}, \quad \lim_{t\to\infty} \psi_n(t) = 0, \quad \int_0^\infty \psi_n(t)\,\mathrm{d}t = \frac{1}{n}. \tag{46}$$

Figure 2 shows ψ_n for various n.

Analytical expressions have been obtained for the functions ξ_n (see reference [17] for details):

$$\xi_0(t) = 2t + 2\sum_{k=1}^{\infty} \frac{\sin \omega_k^0 t}{\omega_k^0}, \tag{47}$$

$$\xi_n(t) = 2\sum_{k=1}^{\infty} \frac{\omega_k^n}{(\omega_k^n)^2 - n^2} \sin(\omega_k^n t), \quad n \geqslant 1, \tag{48}$$

where ω_k^n is the kth positive zero of the first derivative of the Bessel function of order n. It has been shown that the series (47) and (48) converge not everywhere, in particular, that for even n,

$$\xi_n(t) = \begin{cases} +\infty & \text{at } t = 2(4l+1),\ l = 0,\ 1,\ \ldots\ (t = 2,\ 10,\ 18,\ \ldots\ ), \\ -\infty & \text{at } t = 2(4l+3),\ l = 0,\ 1,\ \ldots\ (t = 6,\ 14,\ 22,\ \ldots\ ), \end{cases} \tag{49}$$

and for odd n,

$$\xi_n(t) = \begin{cases} +\infty & \text{at } t = 2(4l+3),\ l = 0,\ 1,\ \ldots\ (t = 6,\ 14,\ 22,\ \ldots\ ), \\ -\infty & \text{at } t = 2(4l+1),\ l = 0,\ 1,\ \ldots\ (t = 2,\ 10,\ 18,\ \ldots\ ). \end{cases} \tag{50}$$

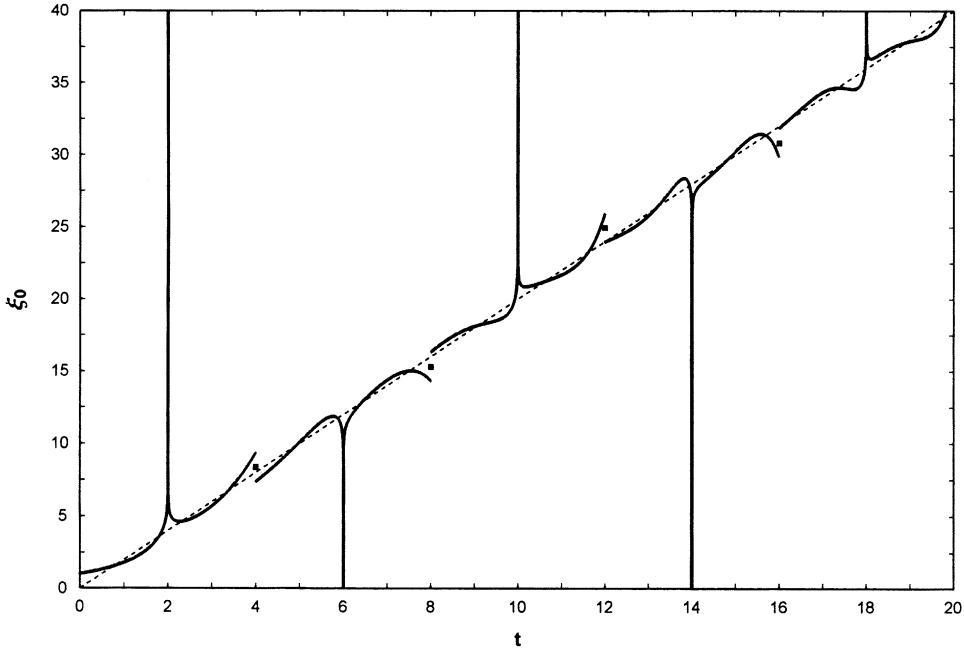

Figure 3. Function $\xi_0(t)$.

It is also worth noticing that

$$\xi_n(t)|_{t=4m} = \left.\frac{\xi_n(t^+) + \xi_n(t^-)}{2}\right|_{t=4m}, \quad m = 1, 2, \ldots, \tag{51}$$

where $\xi_n(t^-) = \lim_{p \to t\,(p<t)} \xi_n(p)$ and $\xi_n(t^+) = \lim_{p \to t\,(p>t)} \xi_n(p)$.

Figures 3 and 4 shows ξ_{mn} for various n. All the above-addressed singular behavior is especially clear for ξ_0.

5. DISPLACEMENTS AND STRESSES

If we expand the displacements as

$$u(x, \theta, t) = \sum_{m=0}^{\infty} \sum_{n=0}^{\infty} u_{mn}(t) \sin(\bar{m}x) \cos(n\theta), \tag{52}$$

$$v(x, \theta, t) = \sum_{m=0}^{\infty} \sum_{n=0}^{\infty} v_{mn}(t) \cos(\bar{m}x) \sin(n\theta), \tag{53}$$

$$w(x, \theta, t) = \sum_{m=0}^{\infty} \sum_{n=0}^{\infty} w_{mn}(t) \cos(\bar{m}x) \cos(n\theta), \tag{54}$$

and substitute the harmonics $u_{mn}(t) \sin(\bar{m}x) \cos(n\theta)$, $v_{mn}(t) \cos(\bar{m}x) \sin(n\theta)$, and $w_{mn}(t) \cos(\bar{m}x) \cos(n\theta)$ into equations (16) and (17), we will arrive at

$$\varepsilon_1 = \bar{m} u_{mn}, \quad \varepsilon_2 = v_{mn} n - w_{mn}, \quad \Omega = -(v_{mn} \bar{m} + u_{mn} n), \tag{55}$$

$$\kappa_1 = -w_{mn} \bar{m}, \quad \kappa_2 = -(w_{mn} n^2 + v_{mn} n), \quad \tau = \bar{m}(w_{mn} n + v_{mn}), \tag{56}$$

where the sine and cosine factors are omitted.

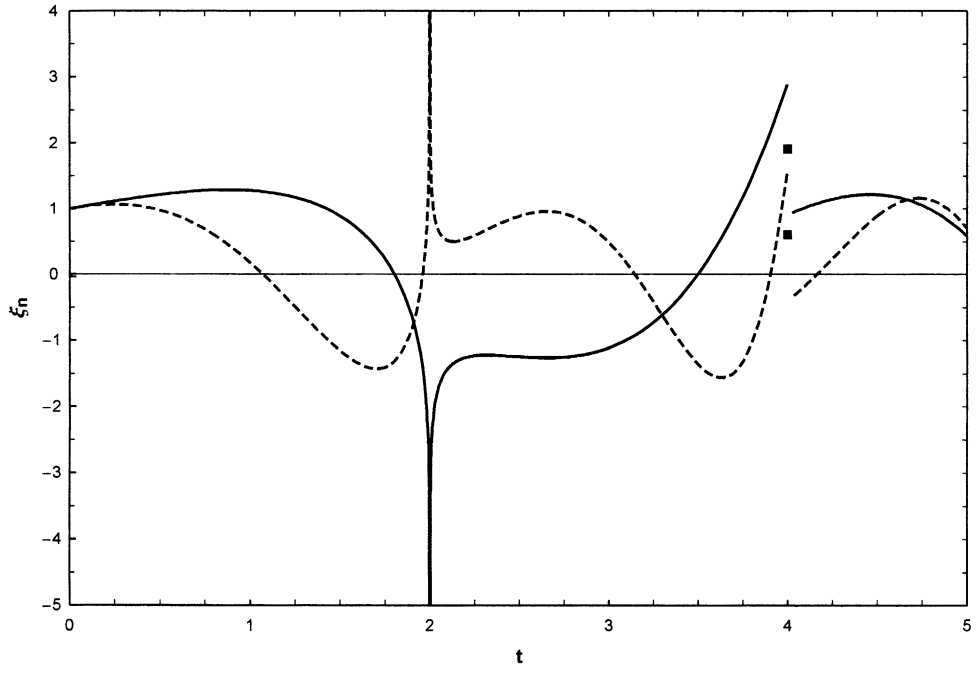

Figure 4. Functions $\xi_1(t)$ and $\xi_2(t)$: ——, $\xi_1(t)$; – – –, $\xi_2(t)$.

Now, if we rewrite the expressions for the strain and kinetic energies (4) and (5) in terms of u_{mn}, v_{mn}, and w_{mn}, perform integration over the shell surface, apply Hamilton's principle, and then incorporate the pressure term p_{mn} given by equation (42), the following integral–differential system can be obtained for every combination of m and n

$$\begin{aligned}
&\gamma^2 \ddot{u}_{mn} + c_{mn}^{11} u_{mn} + c_{mn}^{12} v_{mn} + c_{mn}^{13} w_{mn} = 0,\\
&\gamma^2 \ddot{v}_{mn} + c_{mn}^{21} u_{mn} + c_{mn}^{22} v_{mn} + c_{mn}^{23} w_{mn} = 0,\\
&\gamma^2 \ddot{w}_{mn} + c_{mn}^{31} u_{mn} + c_{mn}^{32} v_{mn} + c_{mn}^{33} w_{mn} = \chi p_{mn},
\end{aligned} \tag{57}$$

where

$$\begin{aligned}
&c_{mn}^{11} = \frac{1-\nu}{2} n^2 + \bar{m}^2,\ c_{mn}^{12} = \frac{1+\nu}{2} \bar{m}n,\ c_{mn}^{13} = c_{mn}^{31} = -\nu\bar{m},\\
&c_{mn}^{21} = \frac{1+\nu}{2} \bar{m}n,\ c_{mn}^{22} = \frac{1-\nu}{2} \bar{m}^2 + n^2 + k^2(n^2 + 2(1-\nu)\bar{m}^2),\\
&c_{mn}^{23} = c_{mn}^{32} = -n + k^2(n^3 + (2-\nu)n\bar{m}^2),\ c_{mn}^{33} = 1 + k^2(\bar{m}^2 + n^2)^2,
\end{aligned} \tag{58}$$

$\gamma = c_s^{-1}$, $\chi = (\bar{\rho}_s c_s^2 h_0)^{-1}$, and the initial conditions are zero.

System (57) has been treated numerically using the finite difference approximation. Series (52)–(54) show reasonably good convergence. However, one should note that the number of terms that must be taken into account with respect to m is at least four times larger than that with respect to n.

The dimensionless stresses in the middle surface of the shell are

$$\sigma_{11} = \frac{\bar{E}}{1-\nu^2}\left(\frac{\partial u}{\partial x} + \nu\frac{\partial v}{\partial \theta} - \nu w\right), \tag{59}$$

$$\sigma_{22} = \frac{\bar{E}}{1 - \nu^2}\left(\frac{\partial v}{\partial \theta} - w + \nu\frac{\partial u}{\partial x}\right), \tag{60}$$

$$\sigma_{12} \equiv \sigma_{21} = \frac{\bar{E}}{2(1 + \nu)}\left(\frac{\partial v}{\partial x} + \frac{\partial u}{\partial \theta}\right), \tag{61}$$

where σ_{11} is a longitudinal (axial) stress, σ_{22} is a transverse (azimuthal) stress, and σ_{12} is a shear stress. Using equations (52)–(54), it is easy to express the stresses in terms of double Fourier series. Note that a dimensionless stress σ is connected with a dimensional one Σ by the relation $\sigma = \Sigma/(\rho_e c_e^2)$.

6. RESULTS AND DISCUSSION

In this section, we will consider a steel shell filled with oil and submersed in water (dimensionless parameters of the system are as follows: density of the exterior fluid, sound speed in th shell material, and radius of the shell are equal to 1·00, $\bar{\rho}_s = 7{\cdot}80$, $c_s = 3{\cdot}57$, $\bar{\rho}_i = 0{\cdot}90$, $c_i = 0{\cdot}96$, $h_0 = 0{\cdot}01$, $\bar{E} = 99{\cdot}4$, and $\nu = 0{\cdot}30$). We will analyze the influence of two different shock waves: one with a source located in the close proximity of the shell ($d = 1{\cdot}2$), and another with a distant source ($d = 5{\cdot}0$).

6.1. DISPLACEMENTS

The performed analysis shows that the longitudinal displacement u is much smaller than the normal w and the transverse v ones. The displacement v is of the same order as w; however, we will only address w as the most practically interesting parameter. Figures 5 and 6

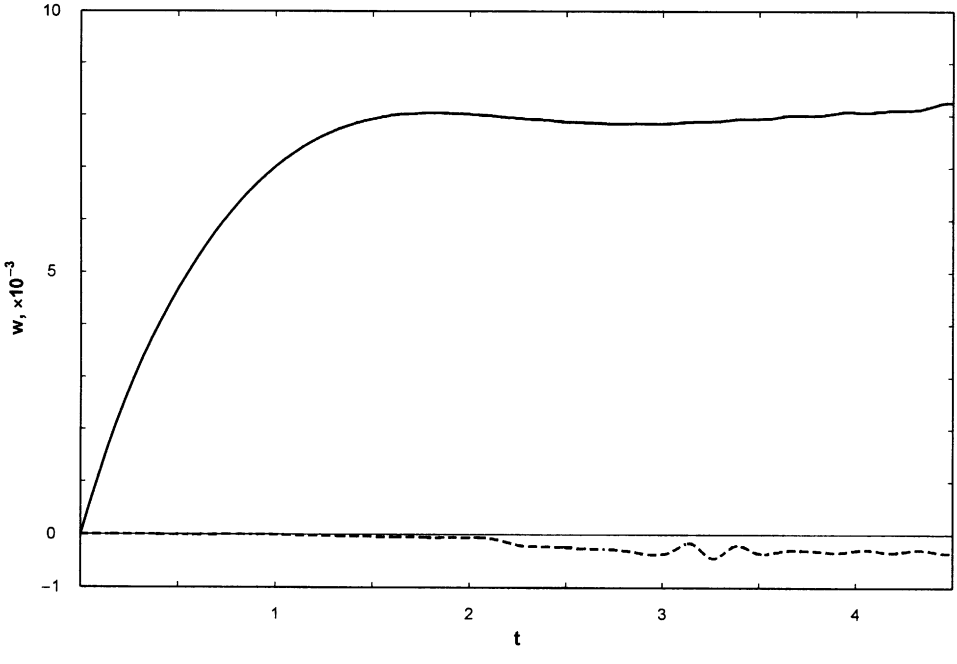

Figure 5. Normal displacement w versus t for $d = 1{\cdot}2$: ——, front point ($x = 0$, $\theta = 0$); – – –, rear point ($x = 0$, $\theta = \pi$).

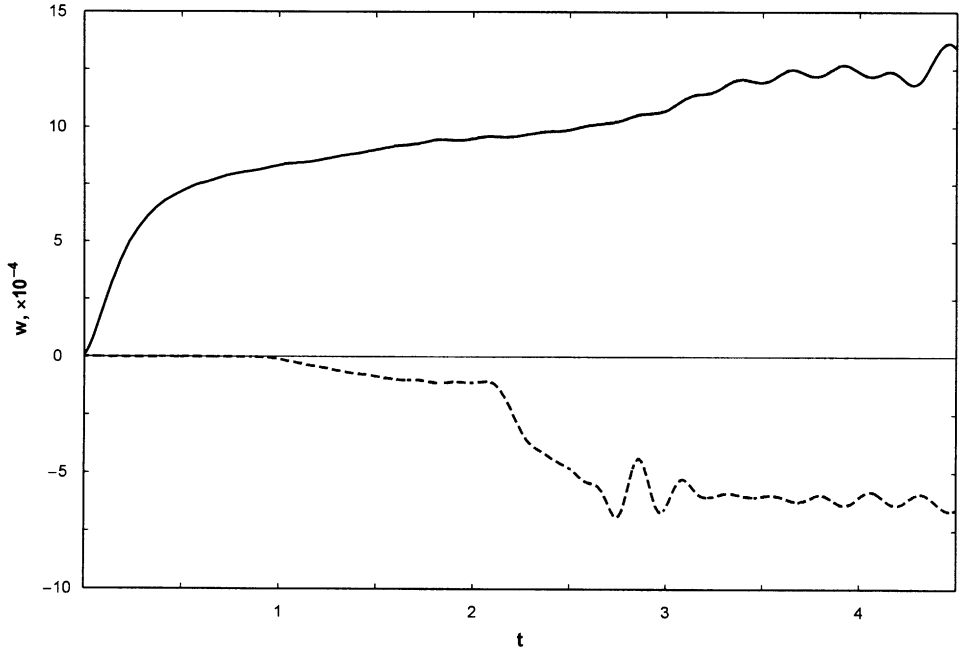

Figure 6. Normal displacement w versus t for $d = 5$: ——, front point ($x = 0$, $\theta = 0$); – – –, rear point ($x = 0$, $\theta = \pi$).

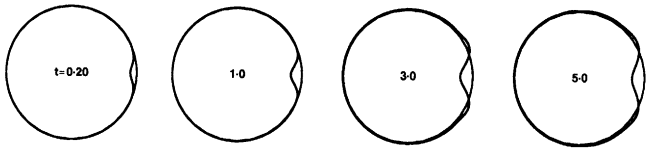

Figure 7. Dynamics of the normal displacement w in the middle cross-section for $d = 1{\cdot}2$.

show w versus t at the front point $x = 0, \theta = 0$ and at the rear point $x = 0, \theta = \pi$. We can see that the maximum deflection in the case of $d = 5$ is about 12% of h_0, and is of order h_0 when $d = 1{\cdot}2$. Thus, the present linear theory can certainly be used for shock waves with a distant source ($d > 2$), and one should be careful dealing with shock waves with a close location of the source ($d < 1{\cdot}5$). Also, it is clear that for $d = 1{\cdot}2$, deflections are localized in the close proximity of the front point, in contrast with the case $d = 5$ when the entire cross-section of the shell experiences considerable deformations. The irregular wave nature of w at $t > 3$ for $d = 5$ is caused by the wave phenomena in the interior fluid, and this issue will be addressed later. Note also that, for the rear point, w is exactly zero during the initial stage of the process (until elastic waves come to the point). This fact is in excellent agreement with a theoretically expected velocity of elastic waves, and validates the correctness of the obtained results.

Figures 7 and 8 show the dynamics of w in the middle cross-section $x = 0$. All the above-noticed effects can be observed more clearly from these figures. Note that the scale of the displacement in the figures does not correspond to the real values and is only aimed to demonstrate the dynamics of the process. The maximum deflection shown in the figures is set to be 20% of the shell radius. The shock wave is propagating from the right to the left. It

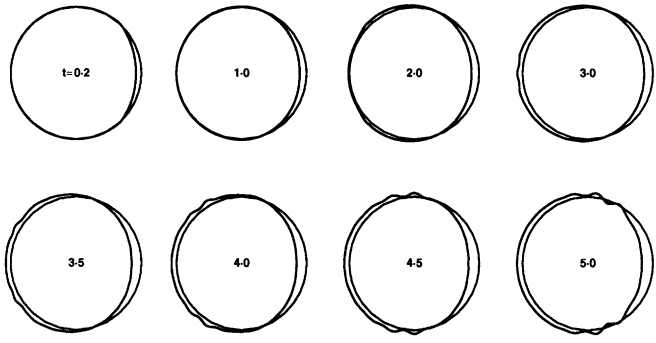

Figure 8. Dynamics of the normal displacement w in the middle cross-section for $d = 5$.

is clear now that for a shock wave with a distant source ($d > 3$) the 'elastic beam' approximation can be more or less successfully used to describe the process. However, for localized loads ($d < 2$) this approximation leads to incorrect results, because only the close proximity of the front point experiences considerable deformation, and no 'beam-like' behavior is observed at all.

6.2. STRESSES

It has been found that the dominant role in forming the stress state belongs to the transverse stress σ_{22}, and this quantity will be addressed in some details. However, the contributions of the shear and axial stresses are also substantial, and those should certainly be taken into consideration. For example, Figure 9 shows the comparison of the longitudinal, transverse, and shear stresses at different points for $d = 5$. One can see that both the longitudinal and shear stresses have considerable magnitude.

Figures 10 and 11 show the dynamics of the transverse stress in the middle cross-section. The compressing stress is shown as 'exterior' and stretching as 'interior'. The shock wave is propagating from the right to the left. The wave effects are especially clear for $d = 5$, so let us now discuss this case. As we can see, during the initial stage of the process the elastic waves are propagating around the shell, and have a constructive superpose at the rear point at $t \approx 1$. Then, the superposed waves are running back in the direction of the front point, where they again superpose constructively at $t \approx 1{\cdot}85$. Meanwhile, at t close to 2 the pressure wave in the interior fluid reaches the rear point, and it affects the stress state dramatically, leading to a large "stretching" peak of the stress at $t \approx 2{\cdot}2$. It causes elastic waves that start to propagate in the direction of the front point, and destructively superpose with the elastic waves propagating in the direction of the rear point. This causes, in turn, a transient state when the stresses are insignificant. This transient state exists for a relatively long time ($t \approx 2{\cdot}5$–4), until the pressure wave in the interior fluid comes to the front point at $t \approx 4$, and causes the 'compressive' peak of the stress at $t \approx 4{\cdot}45$. Then, again, a transient state with insignificant stresses is observed. Note that the last peak of stresses has higher magnitude than the two previous, in spite of the fact that t is large. This clearly shows that early time approximations cannot be used in this case.

One should especially note that the pressure in the shock wave is negligibly small when the transverse stress attains its maximum. Thus, for this case, the maximum stress is driven by the wave phenomena in the interior fluid rather than a direct action of a shock wave. This reiterates the necessity of consideration of all the wave effects both in the shell and the fluids.

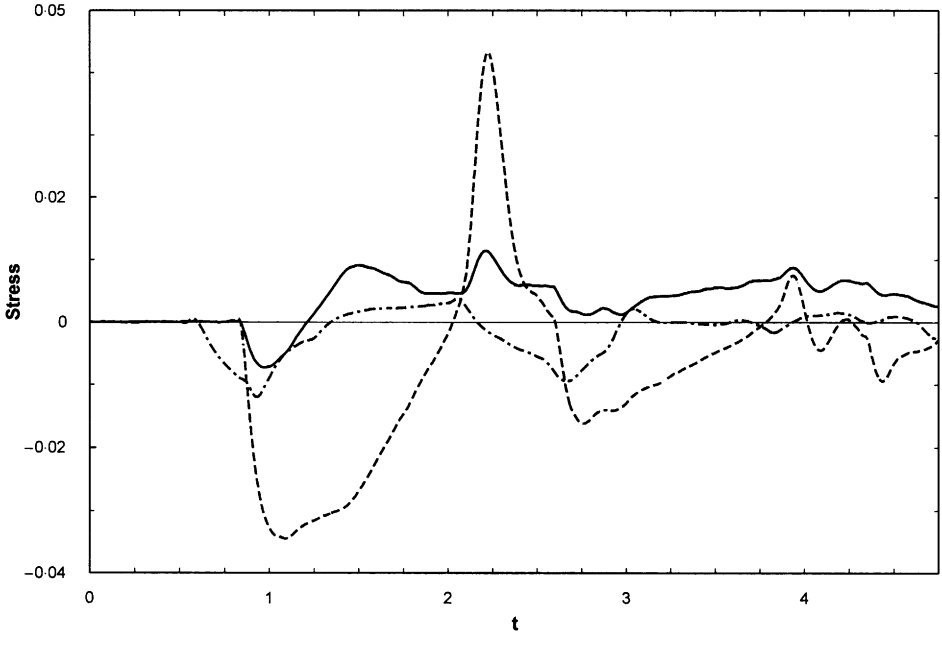

Figure 9. Comparison of the transverse, longitudinal, and shear stresses for the case $d = 5$; ——, longitudinal stress at the point $x = 0$, $\theta = \pi$; – – –, transverse stress at the point $x = 0$, $\theta = \pi$; – · –, shear stress at the point $x = 1{\cdot}6$, $\theta = 0{\cdot}6\pi$.

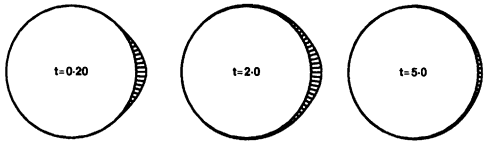

Figure 10. Dynamics of the transverse stress in the middle cross-section for $d = 1{\cdot}2$.

6.3. COMPARISON WITH THE HOLLOW SUBMERGED SHELL

Now we will focus on the difference between a hollow submerged shell and the present case in terms of stress state. The influence that the interior fluid has on the process is the main issue to be discussed here.

Figures 12 and 13 show the transverse stress σ_{22} versus t at the front and rear points for the same (steel) shell submerged in water, the same shock wave with a source located at the distance $d = 5$, but two different cases of contact with an interior fluid (a shell filled with oil and a hallow one). During the initial stage of the process, the behavior of the stresses is the same, and the stress magnitude is much lower for the shell occupied by fluid. However, the stresses become totally different when the wave effects in the interior fluid start to affect the process.

For the front point, this occurs at $t \approx 3$, when the elastic waves initiated at the rear point at $t \approx 2$–$2{\cdot}2$ come to the front point at $t \approx 2{\cdot}9$–$3{\cdot}1$. This causes the first peak of the stress that does not take place for the hollow shell. Then, after a transient state when the stresses are approximately the same for both cases, the wave in the interior fluid, scattered from the domain close to the rear point, comes back to the front point. It causes the second peak at $t \approx 4{\cdot}5$. For the rear point, the stresses start to differ significantly at $t \approx 2{\cdot}2$ when the

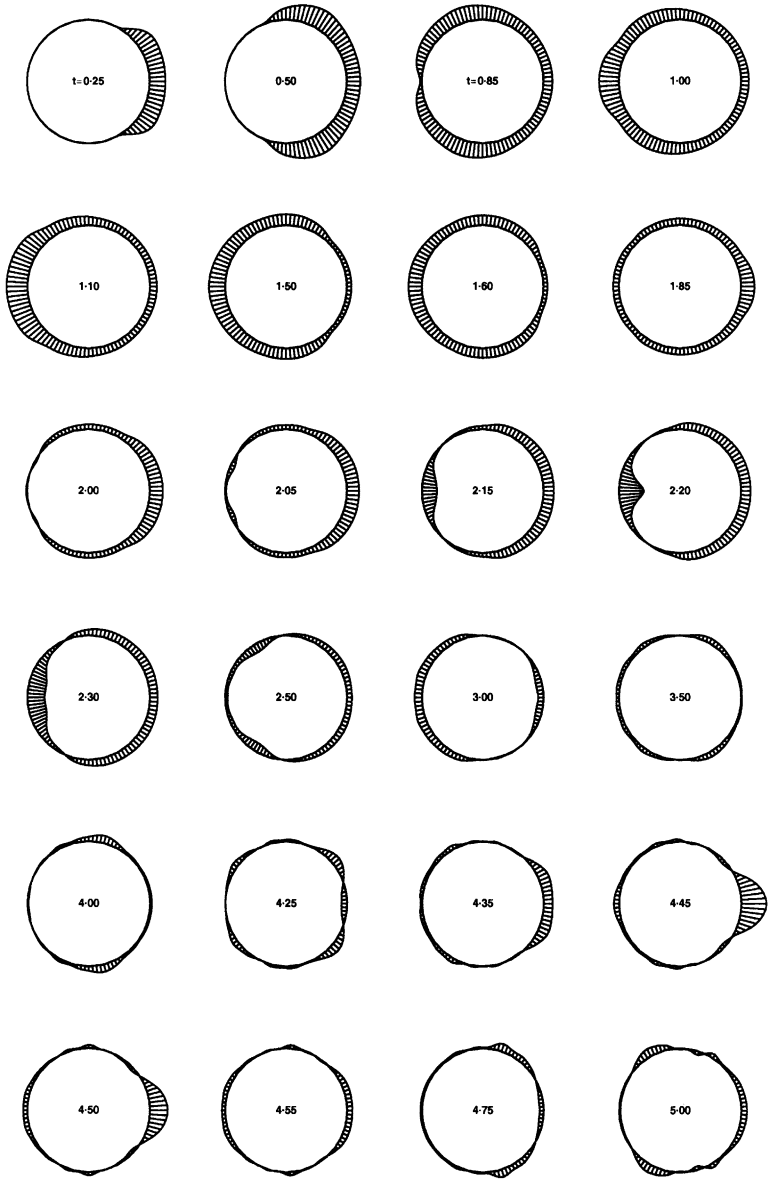

Figure 11. Dynamics of the transverse stress in the middle cross-section for $d = 5$.

pressure wave in the interior fluid comes to that point. Then the stresses become approximately the same for the rest of the process.

Thus, one can see that the case of a shell filled with fluid essentially differs from that of a hollow submerged shell.

7. CONCLUSIONS

In the present paper, the problem of the complete three-dimensional interaction between a spherical shock wave and a fluid-filled submerged circular cylindrical shell is solved

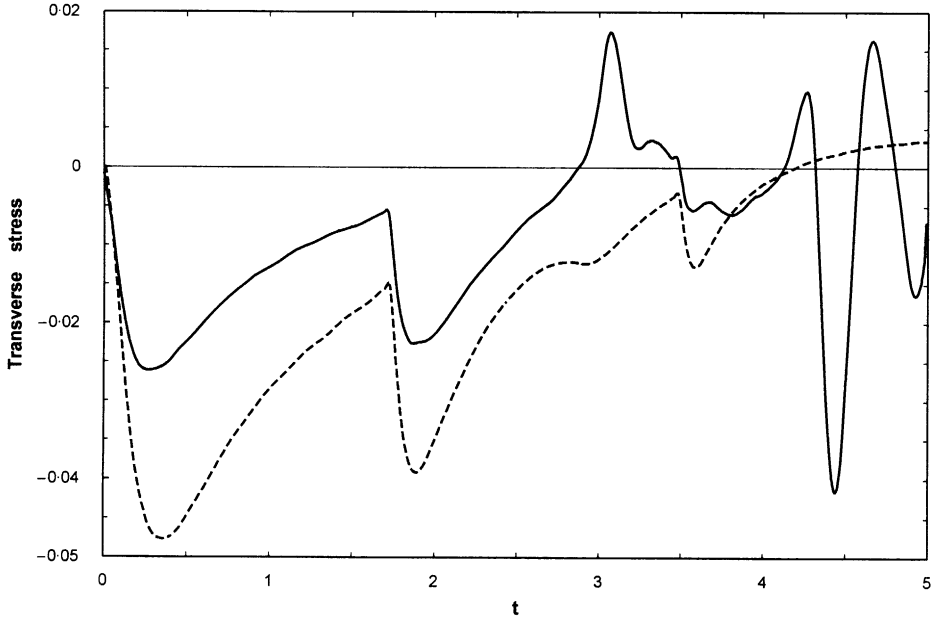

Figure 12. Comparison of the transverse stresses at the front point for $d = 5$: ——, both interior and exterior fluids; – – –, exterior fluid only.

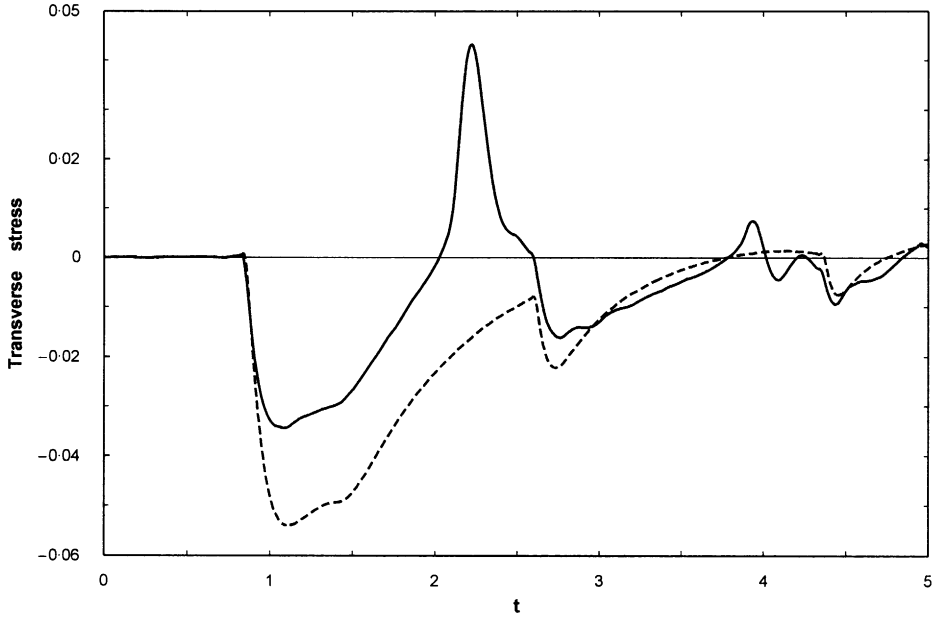

Figure 13. Comparison of the transverse stresses at the rear point for $d = 5$: ——, both interior and exterior fluids; – – –, exterior fluid only.

semi-analytically, and the detail analysis of the stress–strain state of the shell is performed. It has been found that the stress–strain state of the shell has the following features.

(1) The presence of the interior fluid dramatically changes the stress–strain state of the shell. The stress magnitude may attain a maximum not only because of the direct action of

the shock wave or superposition of elastic waves, but also because of wave effects in the interior fluid. It should be noted especially that when the stress maximum is caused by the direct action of a shock wave or the elastic wave superposition, it occurs at $t < 1{\cdot}5$, whereas when it is caused by the wave phenomena in the interior fluid, it occurs at larger times (about 2·2 for the rear point and 4·45 for the front one in the case of a steel shell containing oil and submerged in water). In fact, it seems that for the case of contact with two fluids, it is impossible to precisely predict times when stress magnitude is maximal: it depends on the distance between a shock wave source and the shell, and properties of the involved fluids and shell material. However, it seems that the noticeable influence of wave effects in the interior fluid is much more possible for a shock wave with a distant source. It is also clear now that one should be very careful with the use of early time asymptotics, especially for shock waves with $d > 2$.

(2) The main contribution to the stress state is provided by the transverse stress σ_{22}; however, the longitudinal and shear stresses σ_{11} and σ_{12} have a considerable magnitude as well.

(3) For a shock wave with a source located in the proximity of the shell ($d < 2$) the stress–stain state has a 'local' nature, and there are no effects for the shell as a whole. For shock waves with a distant source ($d > 4$), a substantial domain of the shell is involved in the deformation process, and, as a very rough approximation, one can consider the shell as an elastic beam.

(4) The stress–strain state of the shell has a very complex wave nature, and such wave phenomena as elastic wave interference substantially affect the process, especially stresses. Thus, a very careful analysis has to be performed to ensure taking into consideration all the wave effects.

ACKNOWLEDGMENTS

The author is very grateful to the Killam Trust of Dalhousie University for awarding him the Izaak Walton Killam Memorial Postdoctoral Fellowship. Thanks are also extended to Dr Guy Kember, Department of Engineering Mathematics, Dalhousie University for his useful comments and discussions.

REFERENCES

1. R. D. MINDLIN and H. H. BLEICH 1953 *Journal of Applied Mechanics* **20**, 189–195. Response of an elastic cylindrical shell to a transverse step shock wave.
2. J. H. HAYWOOD 1958 *Quarterly Journal of Mechanics and Applied Mathematics* **11**, 129–141. Response of an elastic cylindrical shell to a pressure pulse.
3. T. L. GEERS 1969 *Journal of Applied Mechanics* **36**, 459–469. Excitation of an elastic cylindrical shell by a transient acoustic wave.
4. H. HUANG 1970 *Journal of Applied Mechanics* **37**, 1091–1099. An exact analysis of the transient interaction of acoustic plane waves with a cylindrical elastic shell.
5. E. N. MNEV and A. K. PERTSEV 1970 *Hydroelasticity of Shells*. Leningrad: Sudostroenie (in Russian).
6. A. K. PERTSEV and E. G. PLATONOV 1987 *Dynamics of Shell and Plates*. Leningrad: Sudostroenie (in Russian).
7. H. HUANG and Y. F. WANG 1970 *Journal of the Acoustical Society of America* **48**, 228–235. Transient interaction of spherical acoustic waves and a cylindrical elastic shell.
8. L. A. PERALTA and S. RAYNOR 1964 *Journal of the Acoustical Society of America* **36**, 476–488. Initial response of a fluid-filled elastic, circular, cylindrical shell to a shock wave in acoustic medium.

9. S.-C. TANG 1965 *Journal of the Engineering Mechanics Division, American Society of Civil Engineers* **37**, 1091–1099. Dynamic response of a tube under moving pressure.
10. W. W. KING and D. FREDERICK 1968 *Journal of the Engineering Mechanics Division, American Society of Civil Engineers* **94**, 1215–1230. Transient elastic waves in a fluidfilled cylinder.
11. R. F. CARPENTER and B. S. BERGER 1972 *Journal of Applied Mechanics* **39**, 682–688. Dynamic response of a semi-infinite elastic cylinder containing an acoustic medium.
12. J. Y. YANG, Y. LIU and H. LOMAX 1987 *American Institute of Aeronautics and Astronautics Journal* **25**, 683–689. Computation of shock wave reflection by circular cylinders.
13. D. DRIKAKIS, D. OFFENGEIM, E. TIMOFEEV and P. VOIONOVICH 1997 *Journal of Fluids and Structures* **11**, 665–691. Computation of non-stationary shock-wave/cylinder interaction using adaptive-grid methods.
14. A. E. H. LOVE 1927 *A Treatise on the Mathematical Theory of Elasticity*. Cambridge: Cambridge University Press.
15. R. H. COLE 1965 *Underwater Explosions*. New York: Dover Publications.
16. S. IAKOVLEV 2001 *Internal report, Dalhousie University*. On the numerical inversion of the Laplace transform for the functions $-K_n(s)/sK'_n(s)$.
17. S. IAKOVLEN 2001 *Internal report, Dalhousie University*. On the response functions of the 'interior' problem of the hydroelasticity of circular cylindrical shells.